

GRB Afterglows from Anisotropic Jets

Z. G. Dai and L. J. Gou

Department of Astronomy, Nanjing University, Nanjing 210093, China

E-mail: daizigao@public1.ptt.js.cn (or dzg@nju.edu.cn)

ABSTRACT

Some progenitor models of gamma-ray bursts (GRBs) (e.g., collapsars) may produce anisotropic jets in which the energy per unit solid angle is a power-law function of the angle ($\propto \theta^{-k}$). We calculate light curves and spectra for GRB afterglows when such jets expand either in the interstellar medium or in the wind medium. In particular, we take into account two kinds of wind: one ($n \propto r^{-3/2}$) possibly from a typical red supergiant star and another ($n \propto r^{-2}$) possibly from a Wolf-Rayet star. We find that in each type of medium, one break appears in the late-time afterglow light curve for small k but becomes weaker and smoother as k increases. When $k \geq 2$, the break seems to disappear but the afterglow decays rapidly. Thus, one expects that the emission from expanding, highly anisotropic jets provides a plausible explanation for some rapidly fading afterglows whose light curves have no break. We also present good fits to the optical afterglow light curve of GRB 991208. Finally, we argue that this burst might arise from a highly anisotropic jet expanding in the wind ($n \propto r^{-3/2}$) from a red supergiant to interpret the observed radio-to-optical-band afterglow data (spectrum and light curve).

Subject headings: gamma-rays: bursts — ISM: jets and outflows — stars: mass loss

1. Introduction

Although the study of gamma-ray bursts (GRBs) has been revolutionized due to observations of their multiwavelength afterglows and particularly due to determinations of their redshifts in the past few years, the question whether the GRB emission is spherical or jet-like has been unsolved. This question has important implications on almost all aspects of the GRB phenomenon, e.g., the total energy that is released in an explosion, the event rate, the physical ejection mechanism and the afterglow decay rate (for a review see Sari 2000).

GRB 990123, the most energetic GRB well-studied, has an isotropic gamma-ray release of $\sim 3.4 \times 10^{54}$ ergs, which corresponds to the rest-mass energy of $\sim 1.9M_{\odot}$ (Kulkarni et al. 1999). From such an energetics, one deduced for the first time that the GRB emission may be highly collimated in this case with a half opening angle of $\theta_m \leq 0.2$ so that the intrinsic explosive energy

could be reduced to $\sim 10^{51} - 10^{52}$ ergs, which is still consistent with the stellar death models, e.g., collapsars (MacFadyen, Woosley & Heger 2000). Another well-known feature of this burst is that its R-band afterglow light curve began to steepen at about day 2 after the burst (Kulkarni et al. 1999; Castro-Tirado et al. 1999; Fruchter et al. 1999). This steepening was first argued to be due to the possibility that a jet has evolved from the spherical-like phase to the sideways-expansion phase (Rhoads 1999; Sari, Piran & Halpern 1999) or that we have observed the edge of the jet (Panaitescu & Mészáros 1999; Mészáros & Rees 1999). Alternative explanation for this steepening was subsequently proposed to be that a shock expanding in a dense medium has undergone the transition from the relativistic phase to the non-relativistic phase (Dai & Lu 1999, 2000). Since then, the dynamics of expanding jets has been numerically studied by many authors (Panaitescu & Mészáros 1999; Moderski, Sikora & Bulik 2000; Huang et al. 2000a, b; Kumar & Panaitescu 2000; Gou et al. 2000; Wei & Lu 2000). Observationally, one marked break has also been observed to appear in the optical afterglow light curves of GRB 990510 (Harrison et al. 1999; Stanek et al. 1999), GRB 991216 (Halpern et al. 2000; Sagar et al. 2000a) and GRB 000301C (Rhoads & Fruchter 2000; Masetti et al. 2000; Jensen et al. 2000; Sagar et al. 2000b; Berger et al. 2000). Holland et al. (2000) recently collected, re-analyzed and explained all of the published photometry for GRB 990123 and GRB 990510. All these studies have assumed that both the energy per unit solid angle and the bulk Lorentz factor at any angle within jets are independent of the angle. Hereafter we refer to such jets as isotropic ones.

In fact, both the energy per unit solid angle ($dE/d\Omega$) and the bulk Lorentz factor within a realistic jet may strongly depend on the angle θ . For example, $dE/d\Omega \propto \theta^{-k}$ where $k \approx 3$ within the energetic jets expected in the collapsar model for GRBs of MacFadyen et al. (2000). We call such jets anisotropic ones. Salmonson (2000) argued that if GRBs arise from anisotropic jets, then the range of the viewing angle (viz., the angle between the line of sight and the jet axis) produces a range in the observed properties of GRBs, i.e. the lag-luminosity relationship. In this paper, we calculate the emission from anisotropic jets expanding both in the interstellar medium (ISM) and in the wind medium. In particular, we consider two kinds of wind: one ($n \propto r^{-3/2}$) possibly from a typical red supergiant star and another ($n \propto r^{-2}$) possibly from a Wolf-Rayet star. To our knowledge, this is the first numerical work about evolution of anisotropic jets and their emission. A preliminary analysis of afterglows from anisotropic jets was made by Mészáros, Rees & Wijers (1998), but our results are different from their analytical ones because we take into account the light travel effects related to different sub-jets within the jet. We also carry out a detailed modelling of the optical afterglow flux data of GRB 991208 given by Sagar et al. (2000a) and Castro-Tirado et al. (2000). Finally, we argue that this burst might arise from a highly anisotropic jet expanding in the wind from a red supergiant to explain the observed radio-to-optical-band afterglow data.

2. The Model

An energetic anisotropic jet is supposed to be ejected in an explosion. We assume that such a jet is adiabatic, i.e., the radiative energy is a negligible fraction of the total energy of the jet. This assumption is valid if the energy density of the electrons accelerated by a shock, produced by the interaction of the jet with its surrounding medium, is a small fraction ϵ_e of the total energy density of the shocked medium or if most of the electrons are adiabatic, i.e., their radiative cooling timescale is larger than that of the jet expansion (Dai, Huang & Lu 1999; Böttcher & Dermer 2000).

2.1. Dynamics

The central question in the next study is how the Lorentz factor γ at angle θ within the jet evolves with the observer time t because all other quantities that appear in the observed flux are functions of γ and of the jet radius and medium density. To obtain γ , we assume that the kinetic energy per unit solid angle within the jet has the following distribution:

$$\varepsilon(\theta) \equiv \frac{dE}{d\Omega} = \begin{cases} \varepsilon_0 & \text{if } \theta \leq \theta_0 \\ \varepsilon_0 \left(\frac{\theta}{\theta_0}\right)^{-k} & \text{if } \theta_0 < \theta < \theta_m, \end{cases} \quad (1)$$

where θ_m is the half opening angle of the jet. The ejected mass per unit solid angle, $M_{\text{ej}}(\theta) = M_0$, is assumed to be independent of the angle (at least over some range of angles). A motivation for this assumption is that a different distribution of the ejected mass affects only evolution of the jet at very early times, but at later times the jet expands based on the Blandford-McKee's (1976) self-similar solution during the relativistic phase and the Sedov-Taylor self-similar solution during the non-relativistic phase. Thus, the initial Lorentz factor at angle θ can be written as

$$\gamma_0(\theta) = \begin{cases} \frac{\varepsilon_0}{M_0 c^2} + 1 & \text{if } \theta \leq \theta_0 \\ \left(\frac{\varepsilon_0}{M_0 c^2}\right) \left(\frac{\theta}{\theta_0}\right)^{-k} + 1 & \text{if } \theta_0 < \theta < \theta_m. \end{cases} \quad (2)$$

The evolution of the Lorentz factor $\gamma(\theta, r)$ can be calculated from the following equation

$$M(r)\gamma^2 + M_0\gamma = M(r) + M_0 + \varepsilon(\theta)/c^2, \quad (3)$$

where $M(r)$ is the mass of the swept-up medium per unit solid angle. Equation (3) expresses the conservation of energy and it applies to only the case without heating of the ejected material by the reverse shock. In this paper we neglect sideways expansion of the jet. Evidence for this consideration is that an observation of GRB 990123 on 7 February 2000 by HST (Fruchter et al. 2000), combined with the previous observations, indicates that the steepening of the R-band afterglow light curve of this burst during a period of ~ 378 days is still roughly consistent with the edge effect of an ultra-relativistic jet of a fixed opening angle expanding in a homogeneous

medium proposed by Mészáros & Rees (1999). Further evidence is that, as argued by Jaunsen et al. (2000), the rapid initial decline, the sharp break in the optical light curve, and the spectral properties of the GRB 980519 afterglow are best interpreted as being due to an ultra-relativistic jet of a fixed opening angle expanding in a wind medium with $n \propto r^{-2}$.

The external medium density is assumed to be a power-law function of radius: $n(r) = Ar^{-s}$, where $A = n_* \times 1 \text{ cm}^{-3}$ for an $s = 0$ (homogeneous) medium (e.g., ISM), $A = 3 \times 10^{35} A_* \text{ cm}^{-1}$ for an $s = 2$ wind possibly from a Wolf-Rayet star as the GRB progenitor (Chevalier & Li 1999, 2000), and $A = 10^{30} \bar{A}_* \text{ cm}^{-3/2}$ for an $s = 3/2$ wind possibly from a typical red supergiant star (Fransson, Lundquist & Chevalier 1996). For convenience, x is defined as the radius r scaled to

$$r_0 = \left[\frac{(3-s)\varepsilon}{m_p c^2 A \gamma_0^2} \right]^{1/(3-s)} = \begin{cases} 2.7 \times 10^{17} \text{ cm } \varepsilon_{53}^{1/3} n_*^{-1/3} \gamma_{0,2}^{-2/3} & \text{if } s = 0 \\ 2.2 \times 10^{16} \text{ cm } \varepsilon_{53} A_*^{-1} \gamma_{0,2}^{-2} & \text{if } s = 2 \\ 4.6 \times 10^{14} \text{ cm } \varepsilon_{53}^{2/3} \bar{A}_*^{-2/3} \gamma_{0,2}^{-4/3} & \text{if } s = 3/2, \end{cases} \quad (4)$$

where $\varepsilon_{53} = \varepsilon(\theta)/10^{53} \text{ ergs}$ and $\gamma_{0,2} = \gamma_0(\theta)/10^2$. Furthermore, we have

$$M(r) = \frac{m_p n(r) r^3}{3-s}, \quad (5)$$

where m_p is the proton mass.

The solution of equation (3) is

$$\gamma(\theta, r) = \frac{1}{2M} \left[\sqrt{M_0^2 + 4M(M + M_0 + \varepsilon/c^2)} - M_0 \right]. \quad (6)$$

The dimensionless radius x and the time t' in the frame comoving with the jet evolve with the observer time t based on

$$\frac{dx}{dt} = \frac{c\beta}{r_0(1-\beta\mu)}, \quad (7)$$

$$\frac{dt'}{dt} = \frac{1}{\gamma(1-\beta\mu)}, \quad (8)$$

where $\beta = \sqrt{1-1/\gamma^2}$, $\mu = \cos\theta$, and the line of sight has been taken to be the jet axis. The solution of equations (7) and (8) combined with (6) gives the dynamics of a sub-jet at angle θ within the jet.

2.2. Synchrotron Radiation

We consider synchrotron radiation of the electrons accelerated by the shock. To calculate the spectrum and light curve, one needs to determine three crucial frequencies: the synchrotron self-absorption frequency (ν'_a), the typical synchrotron frequency (ν'_m) and the cooling frequency (ν'_c). We assume a power law distribution of the electrons accelerated by the shock:

$dn_e/d\gamma_e \propto \gamma_e^{-p}$ for $\gamma_e \geq \gamma_m$, where p is the index of the electron energy distribution and $\gamma_m = [(p-2)/(p-1)](m_p/m_e)\epsilon_e\gamma$ is the minimum Lorentz factor. If ϵ_B is assumed to be the ratio of the magnetic to thermal energy densities of the shocked medium, the magnetic field strength in the shocked medium can be approximated by $B' = [32\pi\epsilon_B\gamma(\gamma-1)nm_p c^2]^{1/2}$.

Under these assumptions, the typical synchrotron frequency can be written: $\nu'_m = \gamma_m^2 e B' / (2\pi m_e c)$. The cooling frequency, $\nu'_c = \gamma_c^2 e B' / (2\pi m_e c)$, is clearly determined by the Lorentz factor γ_c , at which an electron is cooling on the dynamical expansion timescale (t' , measured in the comoving frame). According to Sari, Piran & Narayan (1998), $\gamma_c = 6\pi m_e c / (\sigma_T B'^2 t')$ where σ_T is the Thomson scattering cross-section. Scaled with the typical values of the involved parameters, these two frequencies, measured in the comoving frame, are derived,

$$\nu'_m = \begin{cases} 3.7 \times 10^9 \text{ Hz} \left(\frac{\epsilon_e}{0.1}\right)^2 \left(\frac{\epsilon_B}{0.01}\right)^{1/2} \left(\frac{p-2}{p-1}\right)^2 n_*^{1/2} \gamma^{1/2} (\gamma-1)^{5/2} & \text{if } s = 0 \\ 9.5 \times 10^{10} \text{ Hz} \left(\frac{\epsilon_e}{0.1}\right)^2 \left(\frac{\epsilon_B}{0.01}\right)^{1/2} \left(\frac{p-2}{p-1}\right)^2 \varepsilon_{53}^{-1} A_*^{3/2} \gamma_{0,2}^2 \gamma^{1/2} (\gamma-1)^{5/2} x^{-1} & \text{if } s = 2 \\ 3.7 \times 10^{13} \text{ Hz} \left(\frac{\epsilon_e}{0.1}\right)^2 \left(\frac{\epsilon_B}{0.01}\right)^{1/2} \left(\frac{p-2}{p-1}\right)^2 \varepsilon_{53}^{-1/2} \bar{A}_* \gamma_{0,2} \gamma^{1/2} (\gamma-1)^{5/2} x^{-3/4} & \text{if } s = 3/2; \end{cases} \quad (9)$$

$$\nu'_c = \begin{cases} 2.8 \times 10^{28} \text{ Hz} \left(\frac{\epsilon_B}{0.01}\right)^{-3/2} n_*^{-3/2} \gamma^{-3/2} (\gamma-1)^{-3/2} t'^{-2} & \text{if } s = 0 \\ 1.7 \times 10^{24} \text{ Hz} \left(\frac{\epsilon_B}{0.01}\right)^{-3/2} \varepsilon_{53}^3 A_*^{-9/2} \gamma_{0,2}^{-6} \gamma^{-3/2} (\gamma-1)^{-3/2} x^3 t'^{-2} & \text{if } s = 2 \\ 2.8 \times 10^{16} \text{ Hz} \left(\frac{\epsilon_B}{0.01}\right)^{-3/2} \varepsilon_{53}^{3/2} \bar{A}_*^{-3} \gamma_{0,2}^{-3} \gamma^{-3/2} (\gamma-1)^{-3/2} x^{9/4} t'^{-2} & \text{if } s = 3/2, \end{cases} \quad (10)$$

where t' is in units of 1 s. The synchrotron self-absorption frequency is usually smaller than ν'_m and ν'_c a few hours after the burst. In this case, the optical depth due to synchrotron self-absorption at ν'_a can be approximated by

$$\tau_{ab}(\nu'_a) \approx \frac{5}{3-s} \frac{enr}{B'\gamma_p^5} \left(\frac{\nu'_a}{\nu'_p}\right)^{-5/3} \equiv 1, \quad (11)$$

where $\gamma_p = \min(\gamma_m, \gamma_c)$ and $\nu'_p = \min(\nu'_m, \nu'_c)$ (see, e.g., Panaitescu & Kumar 2000). At early times of the afterglow, all the electrons accelerated behind the shock cool in a timescale smaller than the dynamical expansion timescale of the jet at angle θ , i.e., they are in the fast cooling regime, implying $\nu'_c < \nu'_m$, in which case we find the self-absorption frequency,

$$\nu'_a = \begin{cases} 0.15 \text{ Hz} \left(\frac{\epsilon_B}{0.01}\right)^{6/5} \varepsilon_{53}^{1/5} n_*^{8/5} \gamma_{0,2}^{-2/5} \gamma^{6/5} (\gamma-1)^{6/5} x^{3/5} t' & \text{if } s = 0 \\ 7.5 \times 10^3 \text{ Hz} \left(\frac{\epsilon_B}{0.01}\right)^{6/5} \varepsilon_{53}^{-3} A_*^{24/5} \gamma_{0,2}^6 \gamma^{6/5} (\gamma-1)^{6/5} x^{-3} t' & \text{if } s = 2 \\ 1.3 \times 10^{12} \text{ Hz} \left(\frac{\epsilon_B}{0.01}\right)^{6/5} \varepsilon_{53}^{-7/5} \bar{A}_*^{16/5} \gamma_{0,2}^{14/5} \gamma^{6/5} (\gamma-1)^{6/5} x^{-21/10} t' & \text{if } s = 3/2. \end{cases} \quad (12)$$

At later times, $\nu'_m > \nu'_c$, in which case the self-absorption frequency is given by

$$\nu'_a = \begin{cases} 4.2 \times 10^8 \text{ Hz} \left(\frac{\epsilon_e}{0.1}\right)^{-1} \left(\frac{\epsilon_B}{0.01}\right)^{1/5} \left(\frac{p-2}{p-1}\right)^{-1} \varepsilon_{53}^{1/5} n_*^{3/5} \gamma_{0,2}^{-2/5} \gamma^{1/5} (\gamma-1)^{-4/5} x^{3/5} & \text{if } s = 0 \\ 3.1 \times 10^{10} \text{ Hz} \left(\frac{\epsilon_e}{0.1}\right)^{-1} \left(\frac{\epsilon_B}{0.01}\right)^{1/5} \left(\frac{p-2}{p-1}\right)^{-1} \varepsilon_{53}^{-1} A_*^{9/5} \gamma_{0,2}^2 \gamma^{1/5} (\gamma-1)^{-4/5} x^{-1} & \text{if } s = 2 \\ 3.5 \times 10^{13} \text{ Hz} \left(\frac{\epsilon_e}{0.1}\right)^{-1} \left(\frac{\epsilon_B}{0.01}\right)^{1/5} \left(\frac{p-2}{p-1}\right)^{-1} \varepsilon_{53}^{-2/5} \bar{A}_*^{6/5} \gamma_{0,2}^{4/5} \gamma^{1/5} (\gamma-1)^{-4/5} x^{-3/2} & \text{if } s = 3/2. \end{cases} \quad (13)$$

The synchrotron peak specific luminosity of a ring ($\theta \rightarrow \theta + d\theta$) in the comoving frame is given by

$$dL'_m = \begin{cases} 6.1 \times 10^{29} \text{ ergs s}^{-1} \text{ Hz}^{-1} \left(\frac{\epsilon_B}{0.01}\right)^{1/2} \epsilon_{53} n_*^{1/2} \gamma_{0,2}^{-2} \gamma^{1/2} (\gamma - 1)^{1/2} x^3 \sin \theta d\theta & \text{if } s = 0 \\ 1.6 \times 10^{31} \text{ ergs s}^{-1} \text{ Hz}^{-1} \left(\frac{\epsilon_B}{0.01}\right)^{1/2} A_*^{3/2} \gamma^{1/2} (\gamma - 1)^{1/2} \sin \theta d\theta & \text{if } s = 2 \\ 6.1 \times 10^{33} \text{ ergs s}^{-1} \text{ Hz}^{-1} \left(\frac{\epsilon_B}{0.01}\right)^{1/2} \epsilon_{53}^{1/2} \bar{A}_* \gamma_{0,2}^{-1} \gamma^{1/2} (\gamma - 1)^{1/2} x^{3/4} \sin \theta d\theta & \text{if } s = 3/2. \end{cases} \quad (14)$$

In the case of $\nu'_c < \nu'_m$, the spectrum is (Sari et al. 1998)

$$dL'_{\nu'} = \begin{cases} dL'_m (\nu'_a/\nu'_c)^{1/3} (\nu'/\nu'_a)^2 & \text{if } \nu' < \nu'_a \\ dL'_m (\nu'/\nu'_c)^{1/3} & \text{if } \nu'_a < \nu' < \nu'_c \\ dL'_m (\nu'/\nu'_c)^{-1/2} & \text{if } \nu'_c < \nu' < \nu'_m \\ dL'_m (\nu'_m/\nu'_c)^{-1/2} (\nu'/\nu'_m)^{-p/2} & \text{if } \nu' > \nu'_m. \end{cases} \quad (15)$$

If $\nu'_c > \nu'_m$, the spectrum becomes (Sari et al. 1998)

$$dL'_{\nu'} = \begin{cases} dL'_m (\nu'_a/\nu'_c)^{1/3} (\nu'/\nu'_a)^2 & \text{if } \nu' < \nu'_a \\ dL'_m (\nu'/\nu'_m)^{1/3} & \text{if } \nu'_a < \nu' < \nu'_m \\ dL'_m (\nu'/\nu'_m)^{-(p-1)/2} & \text{if } \nu'_m < \nu' < \nu'_c \\ dL'_m (\nu'_c/\nu'_m)^{-(p-1)/2} (\nu'/\nu'_c)^{-p/2} & \text{if } \nu' > \nu'_c. \end{cases} \quad (16)$$

The observed total flux density at observed frequency ν is given by

$$F_\nu = \int_0^{\theta_m} \frac{dL'_{\nu\gamma(1-\beta\mu)}}{4\pi D_L^2 \gamma^3 (1-\beta\mu)^3}, \quad (17)$$

where D_L is the luminosity distance to the source. For a flat universe with $H_0 = 65 \text{ km s}^{-1} \text{ Mpc}^{-1}$, the luminosity distance to the source $D_L = 2c/H_0(1+z - \sqrt{1+z}) = 1.8 \times 10^{28} \text{ cm}[(1+z)/2]^{1/2}[(\sqrt{1+z} - 1)/(\sqrt{2} - 1)]$.

3. Numerical Results

Integrating equations (7), (8), and (17) numerically, we can easily obtain an afterglow light curve. Figures 1-3 exhibit different afterglow light curves at R-band ($\nu = 4.4 \times 10^{14} \text{ Hz}$) for different k in the homogeneous ISM ($n_* = 1$), in the wind medium with $s = 2$ ($A_* = 1$), and in the wind medium with $s = 3/2$ ($\bar{A}_* = 0.01$), respectively. We choose the remaining parameters: $\epsilon_0 = 10^{53} \text{ ergs sr}^{-1}$, $M_0 = 5 \times 10^{-4} M_\odot \text{ sr}^{-1}$, $\theta_0 = M_0 c^2 / (\epsilon_0 + M_0 c^2) \approx 10^{-2} \text{ rad}$, $\theta_m = 0.3 \text{ rad}$, $p = 2.5$, $\epsilon_e = 0.1$, $\epsilon_B = 0.01$, and $z = 1$. In each figure, the lines from top to bottom correspond to $k = 0, 0.5, 1, 2$ and 3 respectively. From these figures, we can see the following features:

1. At very early times, the afterglow from a jet expanding in the ISM brightens rapidly but the afterglow flux for the wind case is approximately a constant, no matter whether the jet is

isotropic or anisotropic. This may provide a way of distinguishing between the environments as well as GRB progenitors in the near future because rapid, accurate locations of HETE-2 will be able to allow follow-up observations on very early-time X-ray and optical afterglows.

2. For an isotropic jet ($k = 0$) expanding in the ISM, there is a sharp break in the light curve at later times. The time at which this break occurs is close to the analytical result,

$$t_{\text{jet}} \approx 2 \times 10^6 (\varepsilon_{53}/n_*)^{1/3} (\theta_m/0.3)^{8/3} \text{ s}, \quad (18)$$

at which the Lorentz factor of the jet is equal to the inverse of its half opening angle (Mészáros & Rees 1999). But for an isotropic jet expanding in the wind, the break of the light curve is weaker and smoother.

3. In each type of medium, the break of the light curve becomes weaker and smoother as k increases. When $k = 2$ or 3 , the break seems to disappear but the afterglow decays rapidly. This result shows that the emission from expanding, highly anisotropic jets may provide an explanation for some rapidly fading afterglows whose light curves have no break (e.g., GRB 991208; see the next section). We note that in the preliminary analysis of Mészáros et al. (1998), an afterglow decays as one single power-law for any k . The reason for this difference will be discussed in the final section.
4. At very late times, the slopes of the light curves are approximately equal. We also find that the slopes become steeper with the electron distribution index p .

In Figures 4-6 we present the observed radiation spectra computed for a sequence of time for a jet with $k = 3$ in three kinds of medium for the same parameters as in Figures 1-3. It can be seen that even for such an anisotropic jet considered here, the observed radiation spectra can still be divided into four parts, which can be well described from low-energy to high-energy bands by power-law functions $F_\nu \propto \nu^\beta$, with $\beta = 2, 1/3, -(p-1)/2 = -0.75$ and $-p/2 = -1.25$ at $t \geq 10^4$ s, respectively. Two adjacent spectrum portions are still joined very sharply. These results may be due to that the observed radiation spectra are mainly contributed by the $\theta < \theta_0$ part of the jet.

4. The Afterglow of GRB 991208

GRB 991208 was a long burst with a duration of ~ 60 s and a fluence of $\sim 10^{-4}$ erg cm $^{-2}$ (> 25 keV) (Hurley et al. 1999). Its redshift was measured as $z = 0.7055 \pm 0.0005$ (Djorgovski et al. 1999), and thus its isotropic energy in γ -rays is estimated: $E_{\text{iso}} \sim 1.3 \times 10^{53}$ ergs. Because its afterglows at optical, millimeter and radio wavelengths were detected and unusually bright (Sagar et al. 2000a; Castro-Tirado et al. 2000; Galama et al. 2000), a detailed study of this burst may provide new clues regarding the origin of the GRB phenomenon.

Sagar et al. (2000a) gave the observed spectral and temporal indexes of the optical afterglow $\beta_{\text{ob}} = -0.75 \pm 0.03$ and $\alpha_{\text{ob}} = -2.2 \pm 0.1$ while Galama et al. (2000) presented well-sampled spectra

and light curves between radio and millimeter wavelengths for a two-week period, and obtained, for the first time, the evolution of the synchrotron self-absorption frequency $\nu_a \propto t^{-0.15 \pm 0.12}$, the peak frequency $\nu_m \propto t^{-1.7 \pm 0.4}$, and the peak flux density $F_m \propto t^{-0.47 \pm 0.11}$. The existence of one single power law decay for the R-band afterglow implies that the afterglow might be produced by one of the following models: (i) an isotropic jet with sideways expansion, (ii) a relativistic fireball expanding in the ISM, and (iii) a relativistic fireball expanding in the wind. Galama et al. (2000) argued that model (i) can explain the observations, but models (ii) and (iii) are ruled out from α_{ob} and β_{ob} .

If $p = 2.5$, inferred from $\beta_{\text{ob}} = -(p - 1)/2 = -0.75 \pm 0.03$, Figures 7 and 8 provide two good fits to the observed R-band afterglow light curve based on our jet model with $k = 3$ in cases of media (ISM and wind with $s = 2$), respectively. This shows that GRB 991208 might arise from a highly anisotropic jet. However, we note that these two cases may not provide further fits to the observed radiation spectra because the evolution of the theoretical synchrotron self-absorption frequency, peak frequency and peak flux density is inconsistent with the observations by Galama et al. (2000).

Now we assume a generic wind case: $n \propto r^{-s}$. In this case, we have derived the synchrotron self-absorption frequency $\nu_a \propto t^{-3s/[5(4-s)]}$ if $\nu_a < \nu_m$, and the peak frequency $\nu_m \propto t^{-3/2}$, and the peak flux density $F_m \propto t^{-s/(8-2s)}$ in the ultra-relativistic phase (Dai & Lu 1998). If $s = 3/2$, we easily find $\nu_a \propto t^{-0.36}$, $\nu_m \propto t^{-1.5}$, and $F_m \propto t^{-0.3}$. These scaling laws are in approximate accord with those obtained from the observations. This preliminary result prompts us to re-consider a highly anisotropic jet expanding in an $s = 3/2$ wind to fit the afterglow data of GRB 991208. In Figure 9 we first show a satisfactory fit to the observed R-band light curve. It is interesting to note that such a wind has been inferred in the circumstellar medium of SN 1993J (whose progenitor is a red supergiant) by Fransson et al. (1996), and is possibly caused by a variation of the mass-loss rate from the progenitor or by a non-spherical geometry. In Figure 10 we further present a fit to the radio-to-optical-band afterglow spectrum observed on 1999 December 15.5 UT for the same parameters as in Figure 9. Therefore, we can conclude that GRB 991208 might come from a highly anisotropic jet expanding in the wind environment ($s = 3/2$) from a red supergiant.

5. Discussion and Conclusions

The model presented in section 2 clearly includes the following assumptions. First, the initial opening angle of a highly anisotropic jet (e.g., $k = 3$), θ_m , was taken to be 0.3, and the observer's angle (θ_{obs}) between the axis line of the jet and the line of sight to be zero. Because $dL_m \propto \varepsilon(\theta)$ in the ultra-relativistic limit, the emission from the jet mainly arises from the shock-accelerated electrons moving along the axis line. Thus, the flux density of the emission is weakly dependent of θ_m , but strongly depends on θ_{obs} . For example, the flux density at $\theta_{\text{obs}} = 0.3$ is about four orders of magnitude smaller than that of the emission at $\theta_{\text{obs}} = 0$. GRB 980425 was likely such an off-axis burst surrounded by an $s = 2$ wind medium (Nakamura 1999) because its gamma-ray

luminosity of GRB 980425 was also approximately four orders of magnitude smaller than that of GRB 970228/980326 and its X-ray afterglow slowly declined. Second, we considered jets of a fixed opening angle and neglected the effect of sideways expansion based on two observational facts. As shown analytically by Rhoads (1999) and Sari, Piran & Halpern (1999), this effect can lead to a sharp break in an afterglow light curve. However, numerical studies by many authors (e.g, Panaitescu & Mészáros 1999; Moderski, Sikora & Bulik 2000; Huang et al. 2000a, b; Kumar & Panaitescu 2000; Gou et al. 2000; Wei & Lu 2000) show that the actual break, when two effects such as the equal-time surface and detailed dynamics of the jet are considered, is much weaker and smoother than that predicted analytically. Finally, we used the adiabatic solution for kinematics of the jet. This argument is based on the radiative efficiency of the jet, $f = \epsilon_e [t'_{\text{syn}}{}^{-1} / (t'_{\text{syn}}{}^{-1} + t'_{\text{exp}}{}^{-1})]$, defined by Dai et al. (1999). At very early times, the cooling timescale due to synchrotron radiation, t'_{syn} , may be much less than the expansion timescale, t'_{exp} , and $f \approx 0.1(\epsilon_e/0.1)$; but at late times, $t'_{\text{syn}} \gg t'_{\text{exp}}$ and thus $f \approx 0.1(\epsilon_e/0.1)(t'_{\text{exp}}/t'_{\text{syn}}) \ll 1$. Therefore, it can be seen that the energy losses due to synchrotron radiation are insignificant during the whole evolution stage of the jet.

Our numerical results show that for an isotropic jet ($k = 0$) expanding in the ISM, there is a sharp break in the light curve at late times, but for an isotropic jet expanding in the wind, the break of the light curve is weaker and smoother. This result is easily understood in terms of the analytical model of Dai & Lu (1998) and Chevalier & Li (1999, 2000): at early times of the jet evolution, $\gamma > \theta_m^{-1}$, in which stage the jet is spherical-like and thus the decay index of the afterglow $\alpha_1 = -[s/(8 - 2s) + 3(p - 1)/4]$ in the slow cooling regime; but at later times, $\gamma < \theta_m^{-1}$, the decay index becomes $\alpha_2 = -[(6 - s)/(8 - 2s) + 3(p - 1)/4]$ due to the edge effect. These indexes imply the steepening of the light curve $\Delta\alpha \equiv \alpha_1 - \alpha_2 = (3 - s)/(4 - s) = 0.5$ for $s = 2$, 0.6 for $s = 3/2$, or 0.75 for $s = 0$. Therefore, the break in the light curve of the afterglow from a jet expanding in a wind is weaker and smoother than that for a homogeneous medium case. Our results also show that for an anisotropic jet, one break seems to appear in the light curve at small k but becomes weaker and smoother as k increases. This conclusion is different from that presented by Mészáros et al. (1998), who found that an afterglow decays as one single power-law for any k . The reason for this difference is that we took into account the light travel effects related to different sub-jets within the jet but Mészáros et al. (1998) didn't. It is easily understood that an anisotropic jet with a small k can be treated as a quasi-isotropic jet with a half opening angle θ_m , and thus the temporal decay of the flux density of radiation from such a jet will begin to expedite at $t = t_{\text{jet}}$, which is given by equation (18) for the ISM case. However, for a highly anisotropic jet (e.g., $k = 2$ or 3), the contribution of radiation from $\theta > \theta_0$ is in fact much smaller than that from $\theta < \theta_0$ due to the fact that the energy per unit solid angle ($dE/d\Omega$) within this jet decreases rapidly with increasing θ , and thus, the light curve of the resulting radiation should begin to steepen at a very early time, $t \approx 230(\epsilon_{53}/n_*)^{1/3}(\theta_0/10^{-2})^{8/3}$ s, which is also estimated from equation (18) in the ISM case but for θ_m being replaced by θ_0 . Therefore, one cannot see a broken light curve at late times for such a highly anisotropic jet.

In summary, the energy per unit solid angle within a realistic jet may be a power-law function of the angle ($\propto \theta^{-k}$). Such anisotropic jets are expected in the collapsar model of MacFadyen et al. (2000). We numerically calculated light curves and spectra of the emission from anisotropic jets expanding either in the interstellar medium (ISM) or in the wind medium. We also took into account two kinds of wind: one ($n \propto r^{-3/2}$) possibly from a typical red supergiant and another ($n \propto r^{-2}$) possibly from a Wolf-Rayet star. Two of the main results of this work are that (i) at very early times, the afterglow from a jet expanding in the ISM brightens rapidly but the afterglow flux for the wind case is approximately a constant, no matter whether the jet is isotropic or anisotropic. Based on this conclusion, future observations led by HETE-2 on very early-time optical afterglows may be able to distinguish between the environments as well as GRB progenitors. (ii) In each type of medium, one break appears in the late-time afterglow light curve for small k , but becomes weaker and smoother as k increases. When $k \geq 2$, the break seems to disappear but the afterglow decays rapidly. Therefore, one expects that the emission from expanding, highly anisotropic jets provides an explanation for some rapidly fading afterglows whose light curves have no break. We also presented good fits to the optical afterglow flux data of GRB 991208. Finally, to interpret the observed radio-to-optical-band afterglow data of this burst, we argued that it might arise from a highly anisotropic jet expanding in the wind ($n \propto r^{-3/2}$) from a red supergiant.

We would like to thank the referee for several valuable comments that allowed us to improve the manuscript, and D. M. Wei for reading carefully the manuscript. This work was supported by the National Natural Science Foundation of China (grant 19825109) and the National 973 Project.

REFERENCES

- Berger, E. et al. 2000, ApJ, in press (astro-ph/0005465)
- Blandford, R. D., & McKee, C. F. 1976, Phys. Fluids, 19, 1130
- Böttcher, M., & Dermer, C. D. 2000, ApJ, 532, 281
- Castro-Tirado, A. J. et al. 1999, Science, 283, 2069
- Castro-Tirado, A. J. et al. 2000, A&A, submitted
- Chevalier, R. A., & Li, Z. Y. 1999, ApJ, 520, L29
- Chevalier, R. A., & Li, Z. Y. 2000, ApJ, 536, 195
- Dai, Z. G., Huang, Y. F., & Lu, T. 1999, ApJ, 520, 634
- Dai, Z. G., & Lu, T. 1998, MNRAS, 298, 87
- Dai, Z. G., & Lu, T. 1999, ApJ, 519, L155

- Dai, Z. G., & Lu, T. 2000, *ApJ*, 537, 803
- Djorgovski, S. G. et al. 1999, GCN #481
- Fransson, C., Lundquist, P., & Chevalier, R. A. 1996, *ApJ*, 461, 993
- Fruchter, A. S. et al. 1999, *ApJ*, 519, L13.
- Fruchter, A. S. et al. 2000, GCN #712
- Galama, T. J. et al. 2000, *ApJ*, 541, L45
- Gou, L. J., Dai, Z. G., Huang, Y. F., & Lu, T. 2000, *A&A*, in press
- Halpern, J. P. et al. 2000, *ApJ*, in press (astro-ph/0006206)
- Harrison, F. A. et al. 1999, *ApJ*, 523, L121
- Holland, S., Björnsson, G., Hjorth, J., Thomsen, B. 2000, *A&A*, accepted (astro-ph/0010196)
- Huang, Y. F., Dai, Z. G., & Lu, T. 2000b, *MNRAS*, in press
- Huang, Y. F., Gou, L. J., Dai, Z. G., & Lu, T. 2000a, *ApJ*, in press (astro-ph/9910493)
- Hurley, K. et al. 1999, GCN #450
- Jaunsen, A. O. et al. 2000, *ApJ*, in press (astro-ph/0007320)
- Jensen, B. L. et al. 2000, *A&A*, in press (astro-ph/0005609)
- Kulkarni, S. R. et al. 1999, *Nature*, 398, 389
- Kumar, P., & Panaitescu, A. 2000, *ApJL*, in press (astro-ph/0003264)
- MacFadyen, A. I., Woosley, S. E., & Heger, A. 2000, *ApJ*, in press (astro-ph/9910034)
- Masetti, N. et al. 2000, *A&A*, in press (astro-ph/0004186)
- Mészáros, P., & Rees, M. J. 1999, *MNRAS*, 306, L39
- Mészáros, P., Rees, M. J., & Wijers, R. A. M. J. 1998, *ApJ*, 499, 301
- Moderski, R., Sikora, M., & Bulik, T. 2000, *ApJ*, 529, 151
- Nakamura, T. 1999, *ApJ*, 522, L101
- Panaitescu, A., & Mészáros, P. 1999, *ApJ*, 526, 707
- Panaitescu, A., & Kumar, P. 2000, *ApJ*, in press (astro-ph/0003246)
- Rhoads, J. 1999, *ApJ*, 525, 737

- Rhoads, J., & Fruchter, A. S. 2000, ApJ, in press (astro-ph/0004057)
- Sagar, R. et al. 2000a, astro-ph/0003257
- Sagar, R. et al. 2000b, astro-ph/0004223
- Salmonson, J. D. 2000, astro-ph/0010123
- Sari, R. 2000, astro-ph/0002165
- Sari, R., Piran, T., & Halpern, J. P. 1999, ApJ, 519, L17
- Sari, R., Piran, T., & Narayan, R. 1998, ApJ, 497, L17
- Stanek, K. Z. et al. 1999, ApJ, 522, L39
- Wei, D. M., & Lu, T. 2000, ApJ, in press

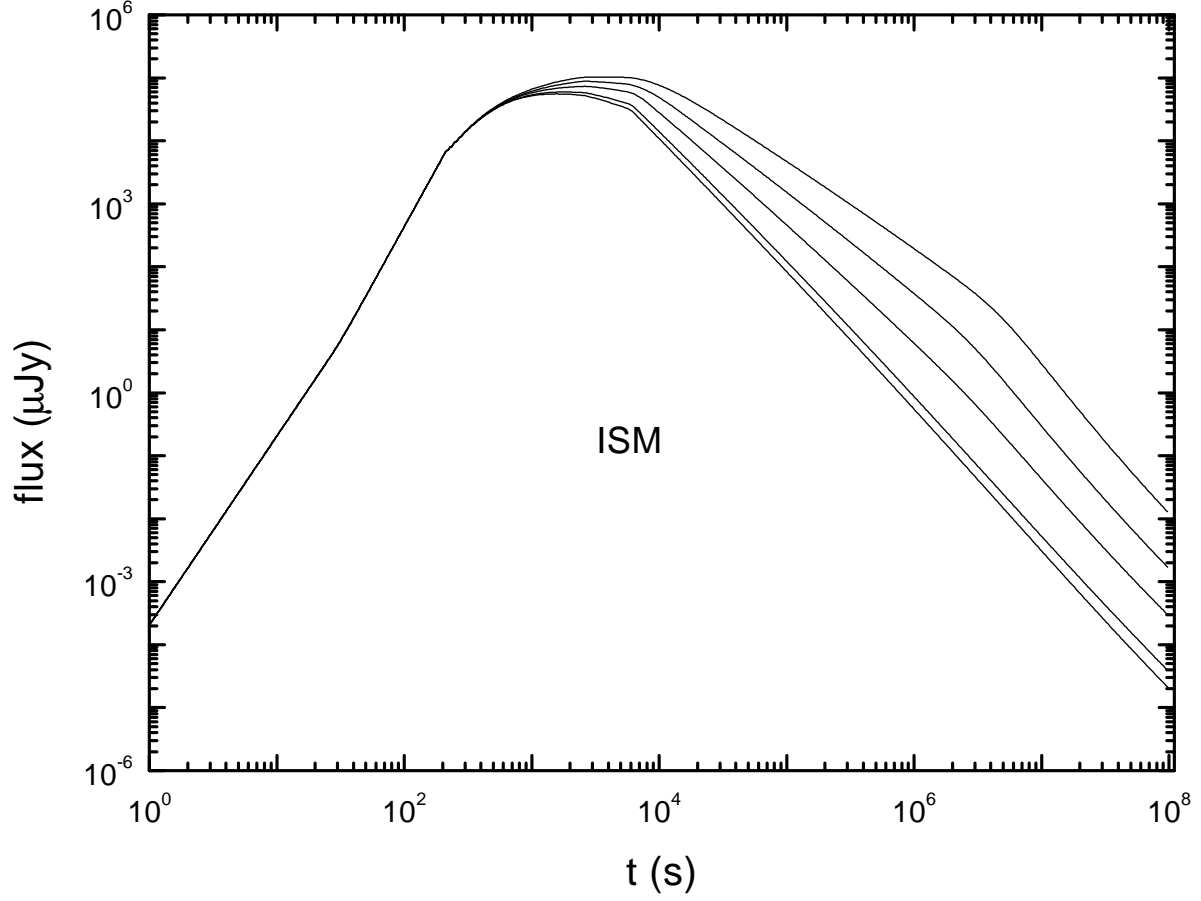


Fig. 1.— Light curves of R-band afterglows from anisotropic jets expanding in the ISM ($s = 0$). The lines from top to bottom correspond to $k = 0, 0.5, 1, 2$ and 3 respectively. The other parameters for the model are seen in the text.

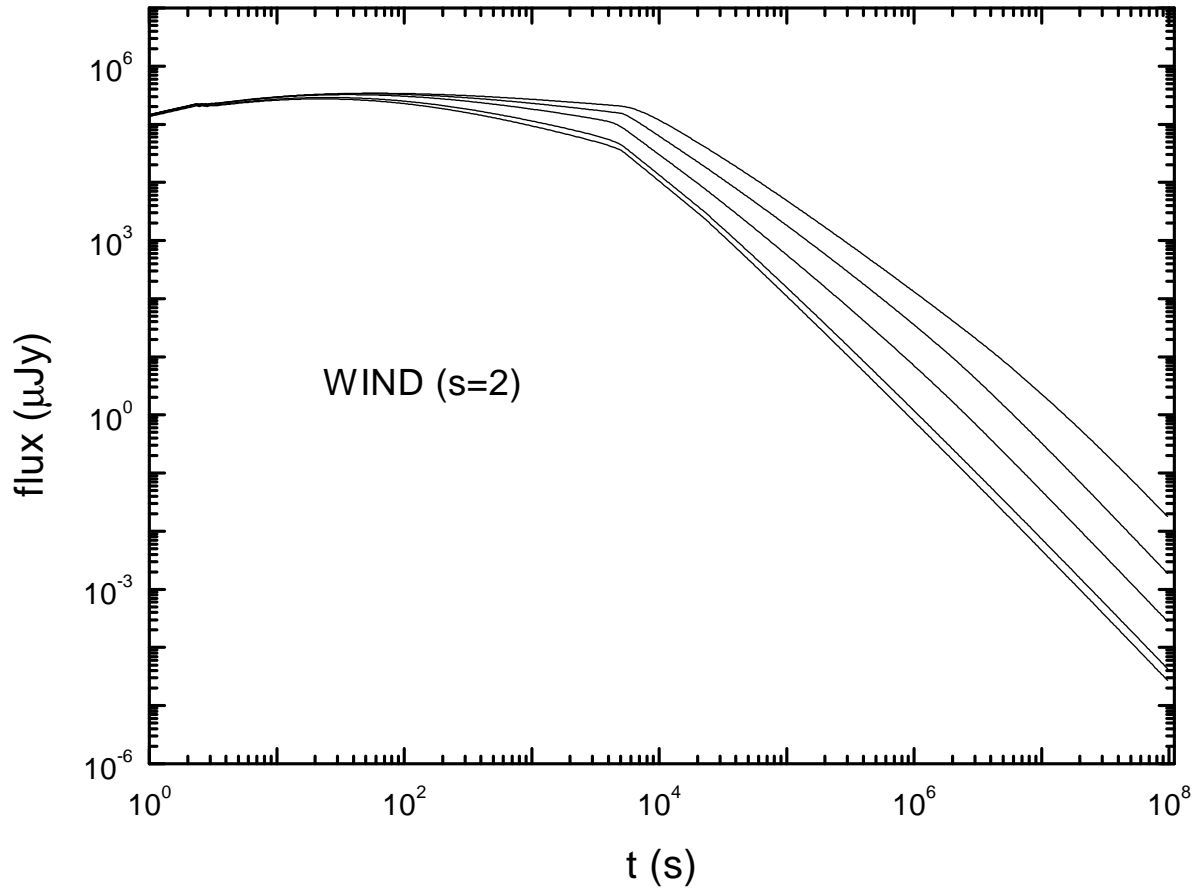


Fig. 2.— The same as in Figure 1 but for the $s = 2$ wind.

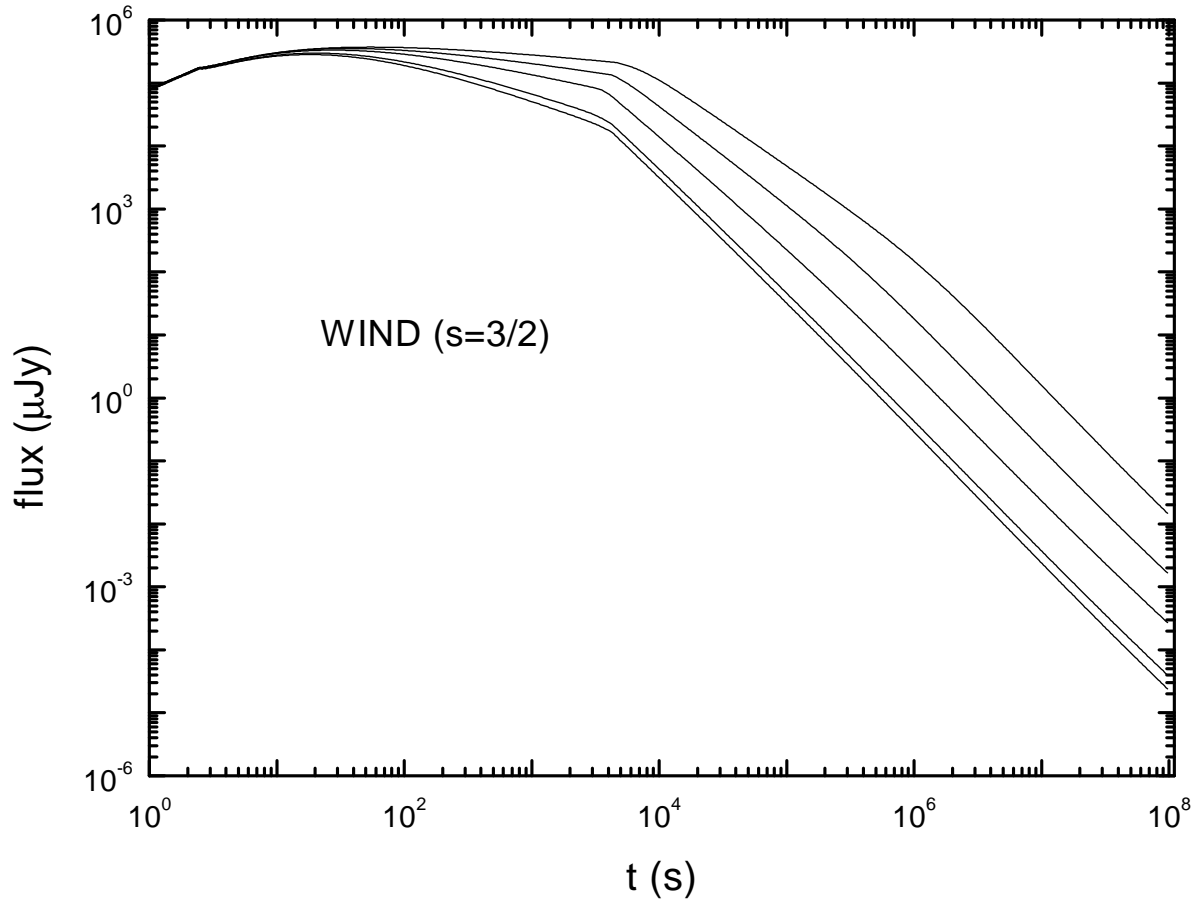


Fig. 3.— The same as in Figure 1 but for the $s = 3/2$ wind.

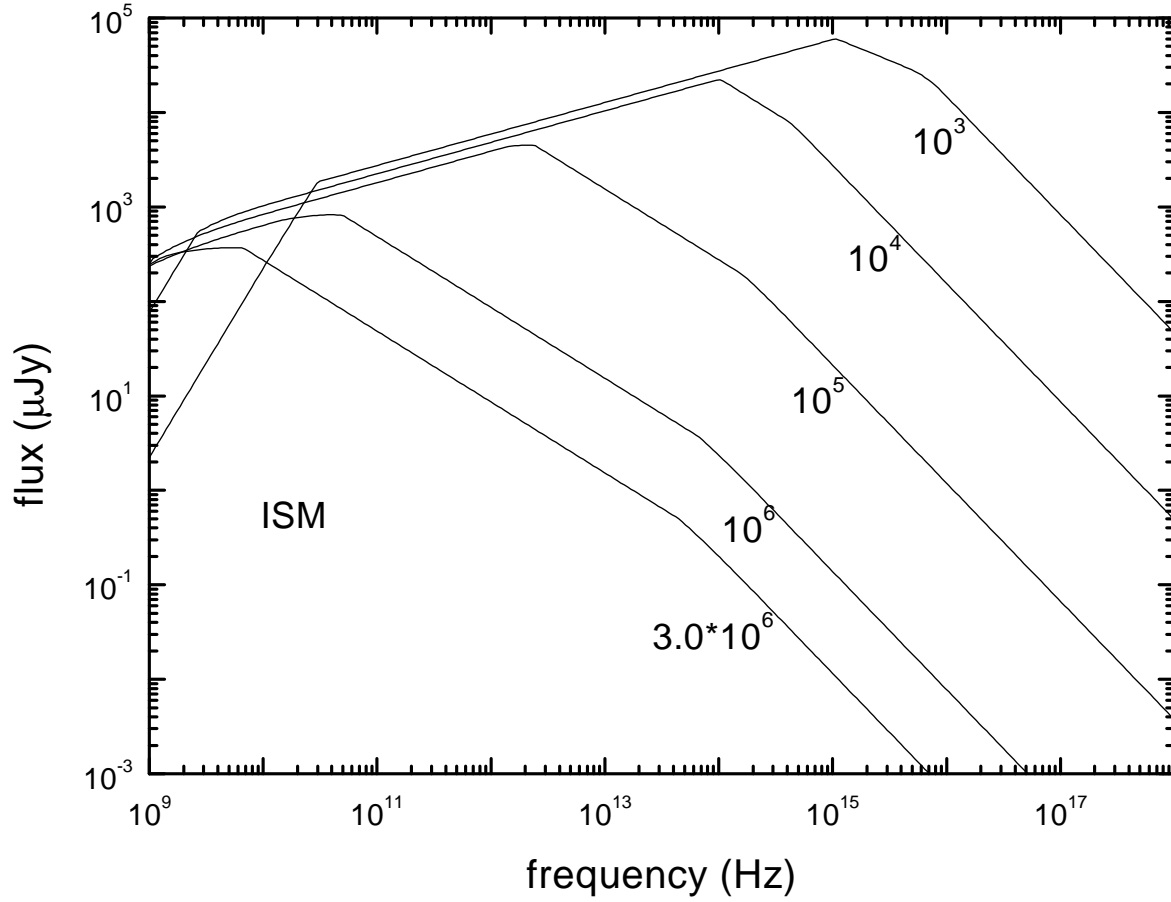


Fig. 4.— Evolution of the observed radiation spectra for a $k = 3$ jet expanding in the ISM ($s = 0$). The numbers mark the observed times in units of second. The other parameters for the model are the same as in Figure 1.

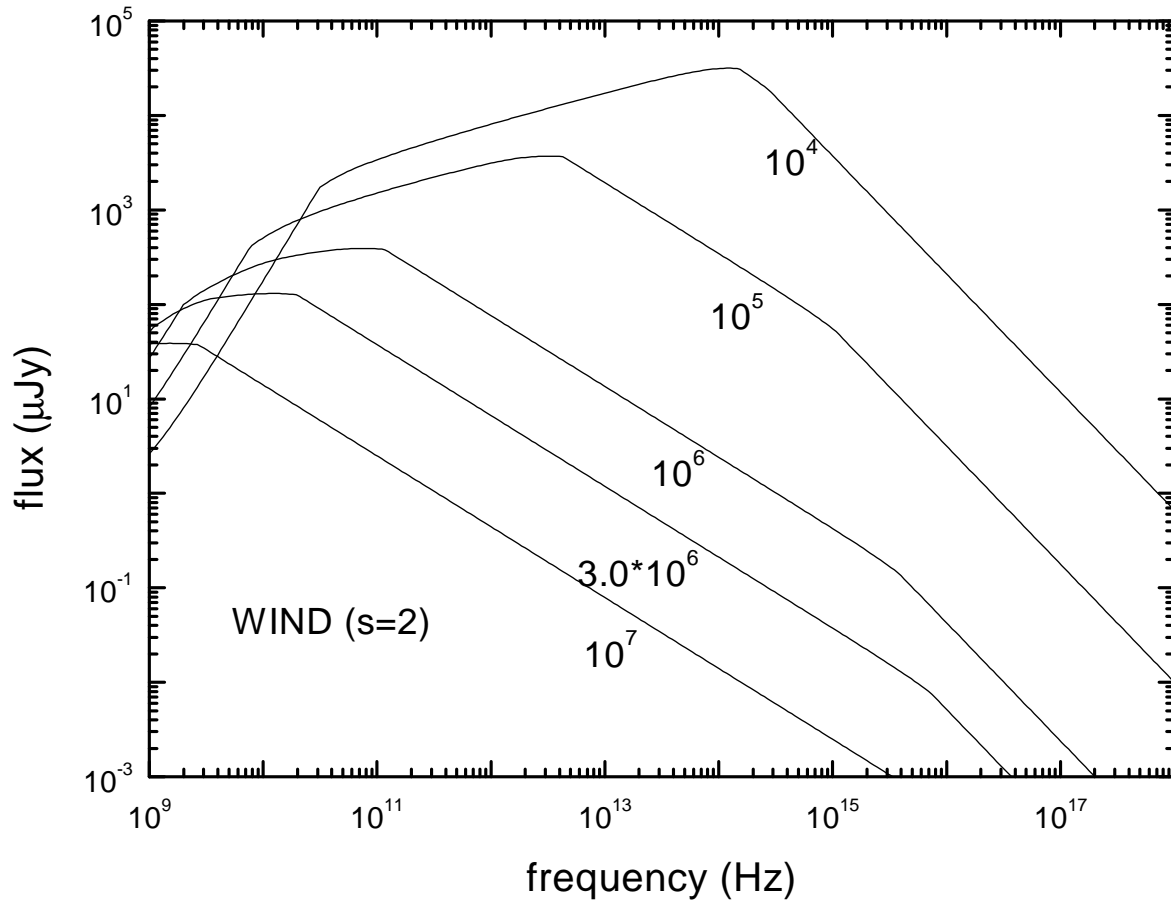


Fig. 5.— The same as in Figure 4 but for the $s = 2$ wind.

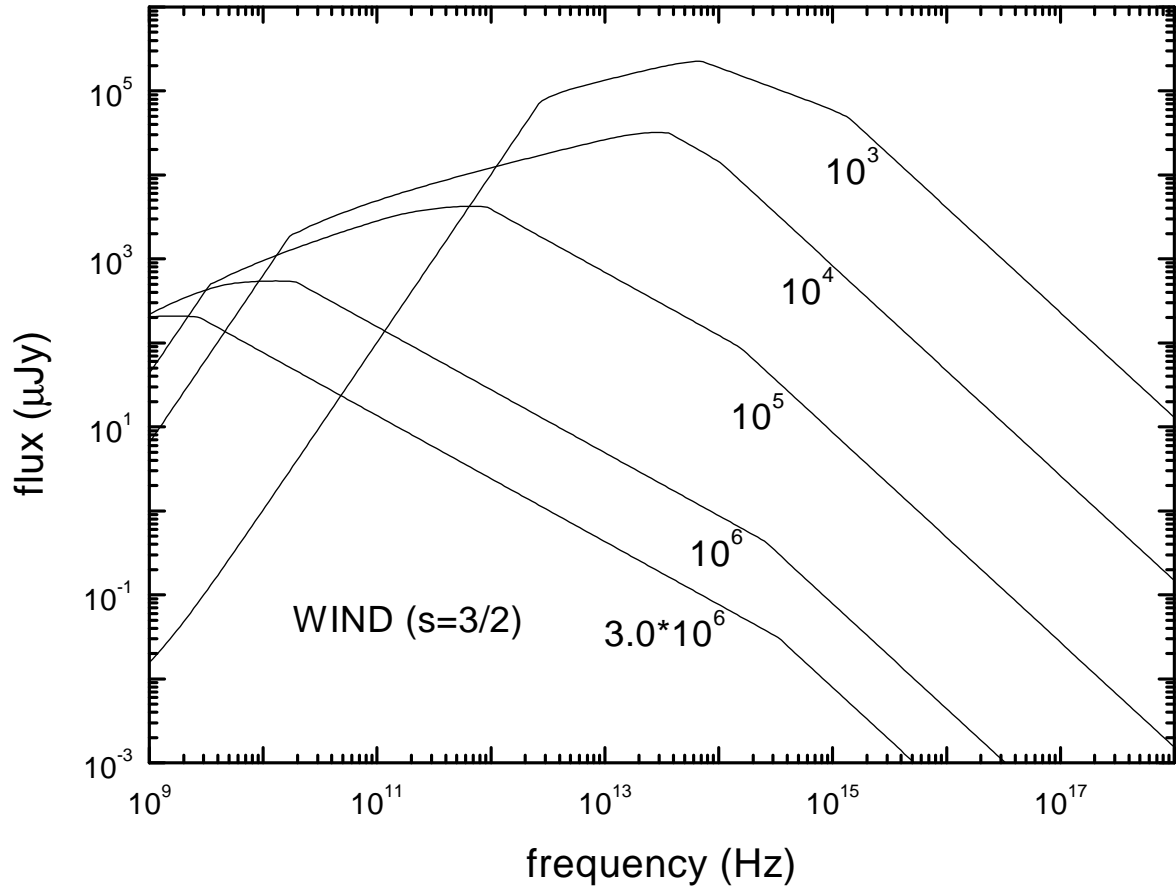


Fig. 6.— The same as in Figure 4 but for the $s = 3/2$ wind.

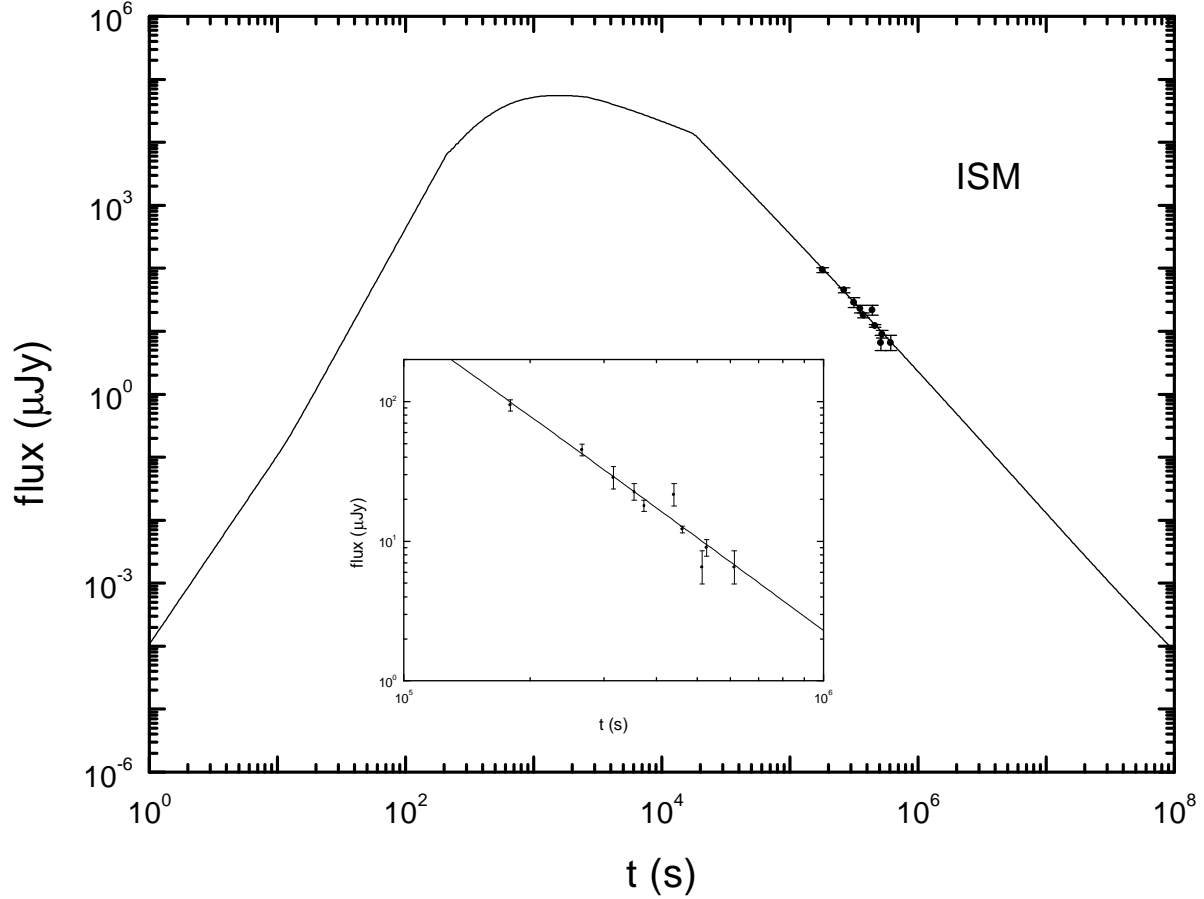


Fig. 7.— Comparison between the observed and theoretically calculated light curves for the R-band afterglow of GRB 991208. The data are taken from Sagar et al. (2000a) and Castro-Tirado et al. (2000), and the model light curve is calculated for a $k = 3$ jet expanding in the ISM ($s = 0$) when an observer is located on the jet axis. The model parameters are chosen: $\epsilon_0 = 10^{53}$ ergs sr^{-1} , $M_0 = 5 \times 10^{-4} M_\odot \text{sr}^{-1}$, $\theta_0 = 10^{-2}$ rad, $\theta_m = 0.3$ rad, $p = 2.5$, $n_* = 1.0$, $\epsilon_e = 0.25$ and $\epsilon_B = 0.01$. The insert shows a clearer fit.

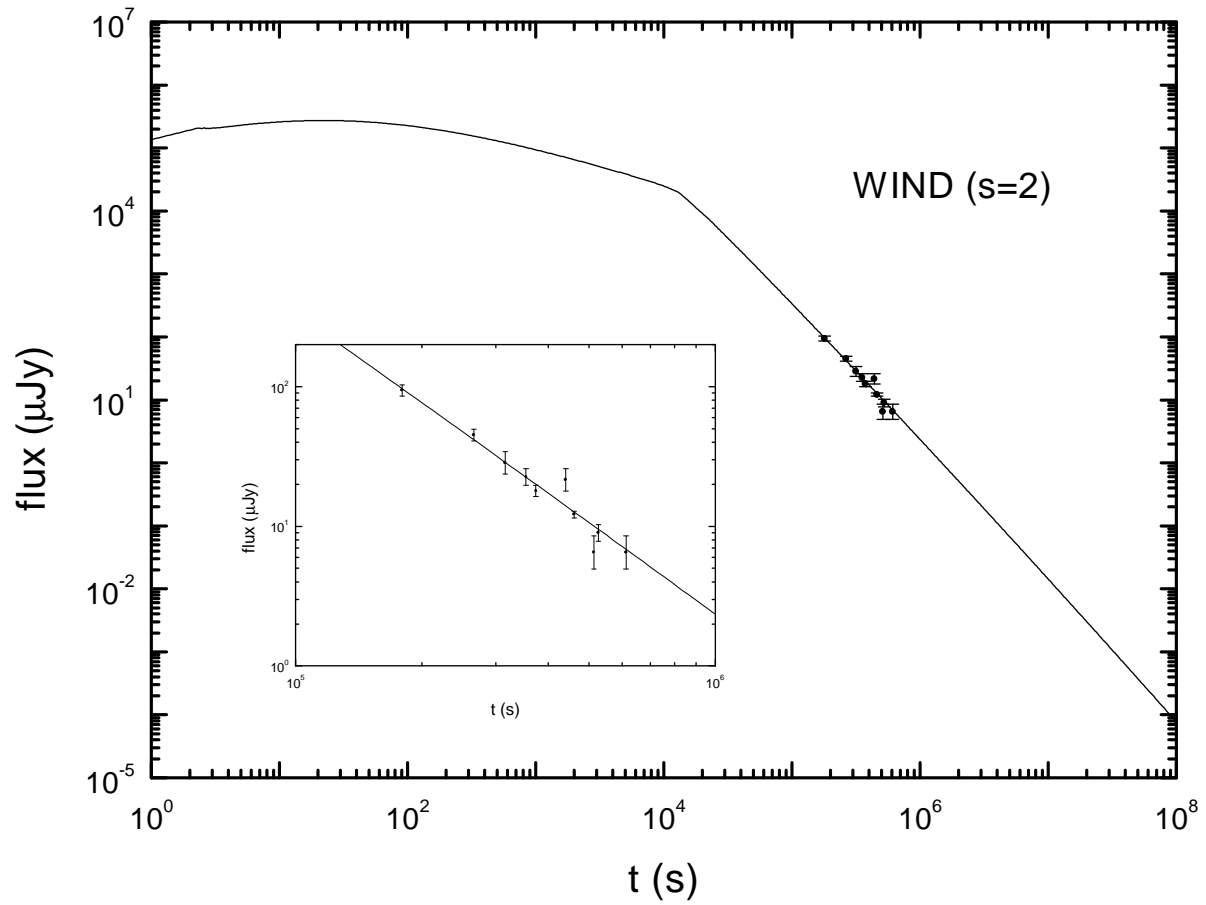


Fig. 8.— The same as in Figure 7 but for $s = 2$ (wind), $A_* = 1.0$ and $\epsilon_e = 0.21$.

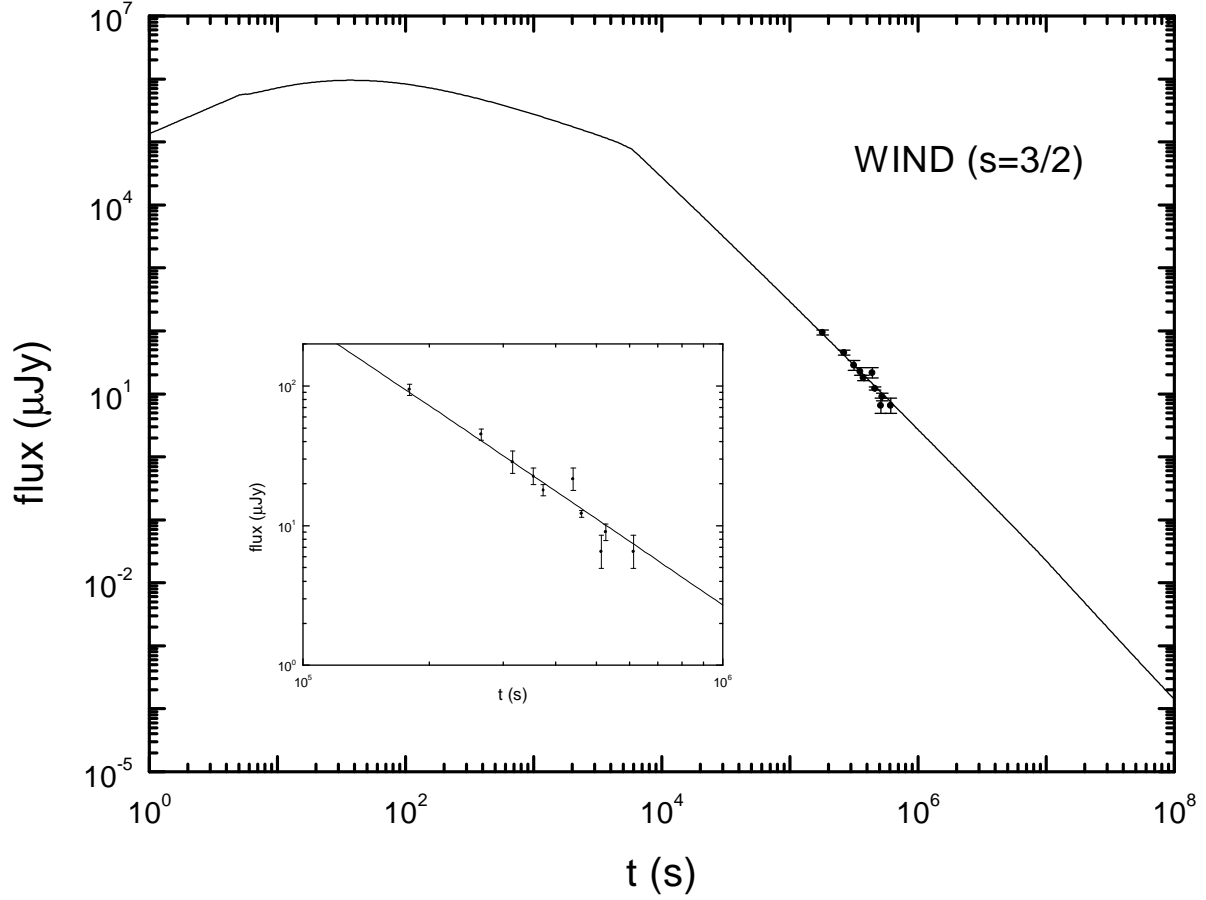


Fig. 9.— The same as in Figure 7 but for the $s = 3/2$ wind case and for the following model parameters: $\epsilon_0 = 1.5 \times 10^{53}$ ergs sr^{-1} , $\theta_0 = 0.01$ rad, $\bar{A}_* = 8 \times 10^{-3}$, $\epsilon_e = 0.16$, $\epsilon_B = 10^{-3}$, $p = 2.5$, $k = 3$, and $\theta_m = 0.3$ rad.

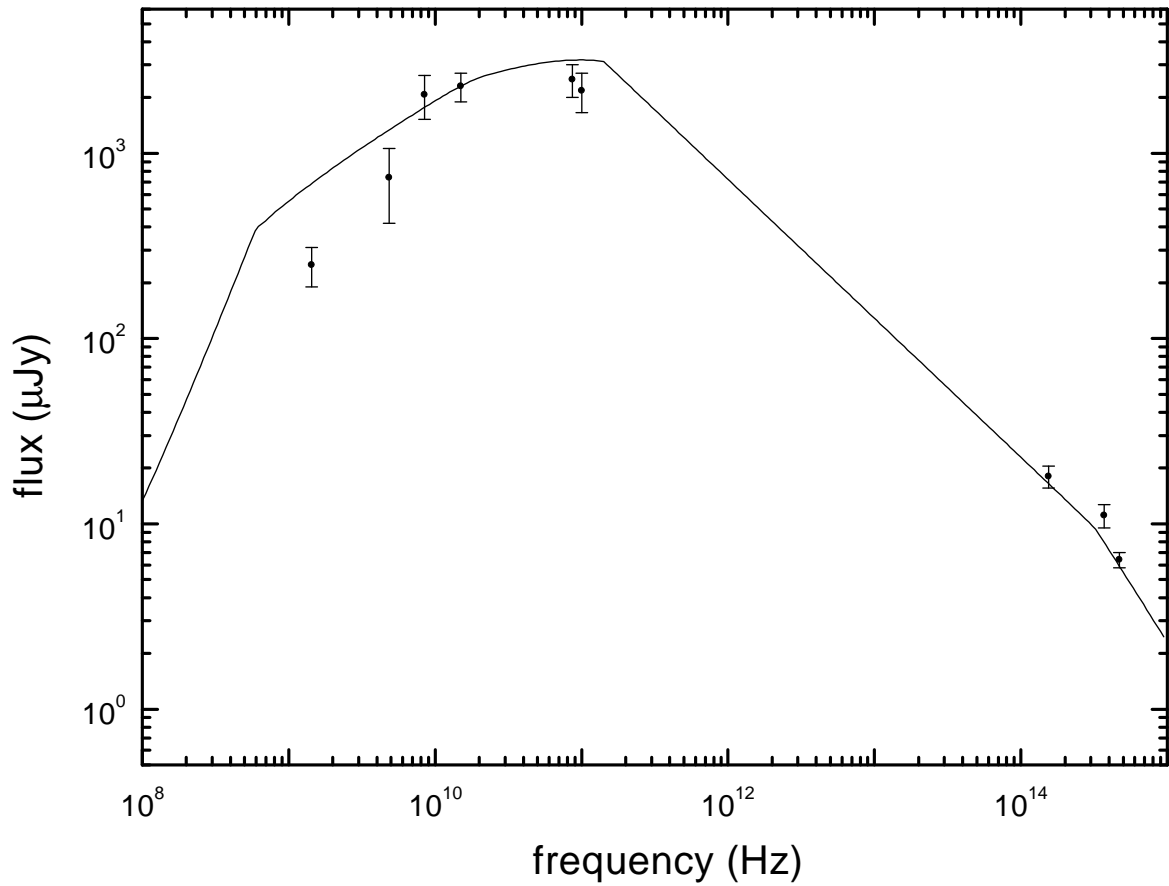


Fig. 10.— Comparison between the observed and theoretically calculated spectra of the GRB 991208 afterglow on 1999 December 15.5 UT. The data are taken from Galama et al. (2000), Sagar et al. (2000a) and Castro-Tirado et al. (2000). The model and its parameters are the same as in Figure 9.